

**This is an electronic reprint of the original article.
This reprint *may differ* from the original in pagination and typographic detail.**

Author(s): Laitinen, Mikko; Sajavaara, Timo

Title: Trajectory bending and energy spreading of charged ions in time-of-flight telescopes used for ion beam analysis

Year: 2014

Version:

Please cite the original version:

Laitinen, M., & Sajavaara, T. (2014). Trajectory bending and energy spreading of charged ions in time-of-flight telescopes used for ion beam analysis. *Nuclear Instruments & Methods in Physics Research. Section B: Beam Interactions with Materials and Atoms*, 325(April), 101-106.
<https://doi.org/10.1016/j.nimb.2014.01.015>

All material supplied via JYX is protected by copyright and other intellectual property rights, and duplication or sale of all or part of any of the repository collections is not permitted, except that material may be duplicated by you for your research use or educational purposes in electronic or print form. You must obtain permission for any other use. Electronic or print copies may not be offered, whether for sale or otherwise to anyone who is not an authorised user.

1
2 **Trajectory bending and energy spreading of charged ions in**
3 **time-of-flight telescopes used for ion beam analysis**
4

5
6 Mikko Laitinen, Timo Sajavaara
7

8
9 Dept. of Physics, P.O.Box 35, FI-40014 University of Jyväskylä, Finland
10

11
12
13 Corresponding author: Mikko Laitinen

14 Telephone : +358 400 994836

15 Fax: +358 14 617 411

16 E-mail: mikko.i.laitinen@jyu.fi
17

18
19
20 **Abstract:**

21 Carbon foil time pick-up detectors are widely used in pairs in ion beam applications as
22 time-of-flight detectors. These detectors are suitable for a wide energy range and for all
23 ions but at the lowest energies the tandem effect limits the achievable time of flight and
24 therefore the energy resolution. Tandem effect occurs when an ion passes the first carbon
25 foil of the timing detector and its charge state is changed. As the carbon foil of the first
26 timing detector has often a non-zero voltage the ion can accelerate or decelerate before
27 and after the timing gate. The combination of different charge state properties before and
28 after the carbon foil now induces spread to the measured times of flight. We have
29 simulated different time pick-up detector orientations, voltages, ions and ion energies to
30 examine the tandem effect in detail and found out that the individual timing detector
31 orientation and the average ion charge state have a very small influence to the magnitude
32 of the tandem effect. On the other hand, the width of the charge state distribution for
33 particular ion and energy in the first carbon foil, and the carbon foil voltage contributes
34 linearly to the magnitude of the tandem effect. In the simulations low energy light ion
35 trajectories were observed to bend in the electric fields of the first timing gate, and the
36 magnitude of this bending was studied. It was found out that 50-150 keV proton
37 trajectories can even bend outside the second timing gate.
38

39
40
41 **Keywords:**

42 tandem effect, carbon foil, Time-of-Flight, ToF-E, ToF-ERDA
43
44

1 Introduction

Time-of-flight (ToF) telescope comprising two carbon foil time pick-up detectors (for short: timing gates) is one of the most versatile and useful detectors in the field of ion beam analysis. It can be used for all ions and usable energy regime extends down to few tens of keVs [1]. The energy resolution of the ToF-system for monoenergetic ions depends from the individual timing accuracy of the detectors, the distance of the flight path, the energy straggling and the thickness variation of the first carbon foil and also from the tandem effect [2], to list a few. The performance of the MCP, anode [3,4] and the isochronous electron transportation [5,6] in the timing gates contribute also to the energy resolution. Another additional factor is the timing gate orientation [7] in which, for example, the forward emitted electrons have increased probability for higher energies in wider emission angles [8] which will lead to non-isochronous electron transportation from the foil to the MCP. The better known limitations of the ToF-detectors are the detection efficiency for hydrogen and low energy heavy ion scattering in the carbon foil [9] of the first timing gate (T1). One additional limitation which comes in question with the tandem effect is the use of high or low voltages: when using the MCP for electron amplification, either the carbon foil or anode needs to be at elevated voltage. If the carbon foil is in high voltage and enhances the tandem effect, then the anode can be grounded. The grounded foil -situation requires an anode in high voltage while it also increases the background events because of the free electrons are then more easily accelerated towards the MCP.

When high depth resolution for thin film sample analyzes is aimed for elastic recoil detection telescopes equipped with ToF it is beneficiary to use lower energies [10]. In lower energies, however, one has to also consider the tandem effect [2] and the bending of the ion trajectories in the electric fields of the first timing gate. The tandem effect can generally be described as a time-of-flight (and energy) spread due to the charge state exchange of the passing ion in the carbon foil of the first timing gate. This phenomenon is often listed as one of the most important factors limiting the resolution of ToF detectors for ion beam analysis using the lowest beam energies [2,10--12]. The additional energy spread of the passing ion caused by the tandem effect has often been written in a form: $\sigma_{\text{tandem}} = \overline{\Delta q} \cdot V_{\text{T1 foil}}$, where $\overline{\Delta q}$ is the average change of the charge of the ions upon their passage through the T1 foil having voltage of $V_{\text{T1 foil}}$. However, further quantification of the $\overline{\Delta q}$ has generally not been explained.

For low energy charged ions also notable bending of ion trajectories takes place in the time pick-up detectors due to electric fields and can even lead to a situation that no ions reach the second timing gate at all if both gates have strictly limited solid angles.

We have simulated with SimION software [13] different timing gate configurations and measured experimentally results with the time-of-flight elastic recoil detection (ToF-ERD) spectrometer in Jyväskylä to test and to gain better knowledge of the ion trajectory bending and the tandem effect. The aim was to find the optimal timing gate design, if not the one used at the moment in the view of bending of ion trajectories and the tandem effect.

91

92 2 Simulation and experimental setups

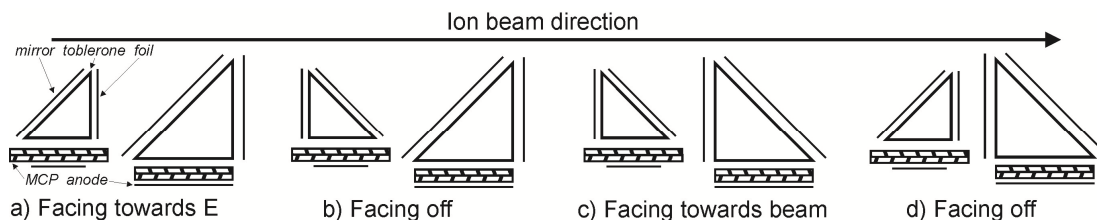
93

94 Simulation software used was SimION [13] which is a 3D capable electron and ion
95 transport simulation program. The time-of-flight telescope dimensions were replicated to
96 the simulation program from the real ToF-ERD system existing in our laboratory. The
97 wire grids in the timing gates were modeled as transparent potential barriers. Similar
98 simplification was applied also to the carbon foils.

99

100 Most important assumption made in this study is that the charge exchange equilibrium is
101 always reached for energetic (>50 keV) ions in both T1 carbon foil ($\sim 3 \mu\text{g}/\text{cm}^2$) and in
102 the sample from which the ions, scattered or recoiled, emerge towards the ToF-E
103 telescope. There are numerous publications detailing with the charge exchange processes
104 for different targets, incident ions and energies but for the essentials, a general illustration
105 of the field is summed well in [14] and a more specific case for lower energies is
106 presented in [15]. In these references it is shown that about $1 \mu\text{g}/\text{cm}^2$ of material is
107 already enough for MeV ions to reach the charge state equilibrium. If this statement is
108 expected to be valid then the charge states of the ions incoming to the first time pick-up
109 detector and leaving from the T1 foil are independent of each other but follow the same
110 energy dependent charge state distribution. This means that for the He ions, for example,
111 there are total 3×3 different charge state combinations for the ions that have emerged
112 from the sample and passed the T1 foil and thus 9 different ToFs can exist after the T1
113 foil for the He ions.

114



115

116 *Figure 1. Different timing gate orientations. In all simulations the distance from foil-to-*
117 *foil was kept the same. The both timing gate carbon foils in a) face towards the E detector,*
118 *in b) face off from each other, in c) face towards the beam and in d) face towards each*
119 *other.*

120 During the simulations, the timing gate orientations (see Fig. 1) and voltages were
121 changed to examine how the transmitted ions behave in different configurations. In
122 simulations, when non-zero voltage was applied to the T1 carbon foil, it was assumed
123 that the incoming ions had scattered/recoiled from a sample in ground potential and
124 reached the charge state equilibrium characteristic for that particular energy. The charge
125 state distributions for different energies were taken from the tables of comprehensive
126 database [16] where different ion-target combinations are summed up from numerous
127 publications from the past decades. For this study, only carbon foil as a target (=T1 foil)
128 material was considered.

129

130 Experimental setup consists of a sample located at the distance of 32 cm from the first
131 timing gate, particle suppressors, two carbon foil time pick-up detectors similar to the
132 design of Busch et al. [6] and with the time-of-flight distance of 62 cm. After the second
133 timing gate there is a silicon energy detector allowing coincident ToF-E measurements
134 and thereafter mass identification of the individual particles. The foils of the both time
135 pick-up detectors in the experimental setup are facing towards the energy detector (like in
136 Fig. 1 a). Typical voltages in the experimental setup are: -500 V for the T1 foil and
137 mirror, +1000 V for the toblerone (which is the triangular part creating a field-free region)
138 and MCP_{in} and +2750 V for the anode; -2800V for the T2 foil and mirror, -1800 V for
139 toblerone and MCP_{in} and 0 V for the anode, similar as shown in the Fig. 2 b).

140

141 **3 Results**

142

143 When the full ToF simulations were run with different ions, two significant results could
144 easily be identified. First was the clear bending of light, low energy ion trajectories in the
145 electric field of the first timing gate mirror grid/harp. The second was the observation that
146 even with zero voltage at the T1 carbon foil, or even at both T1 and T2 foils, the charge
147 state dependent tandem effect did not vanish completely. From the simulations it also
148 became evident that using the existing timing gate configuration of the ToF-E telescope
149 no concrete experimental evidence could be obtained of the tandem effect. This was due
150 to the limited maximum achievable voltage of the T1 foil (~1250 V) in our operating
151 ToF-ERDA configuration. Thus results (all results given are FWHM) presented here are
152 all based on simulations.

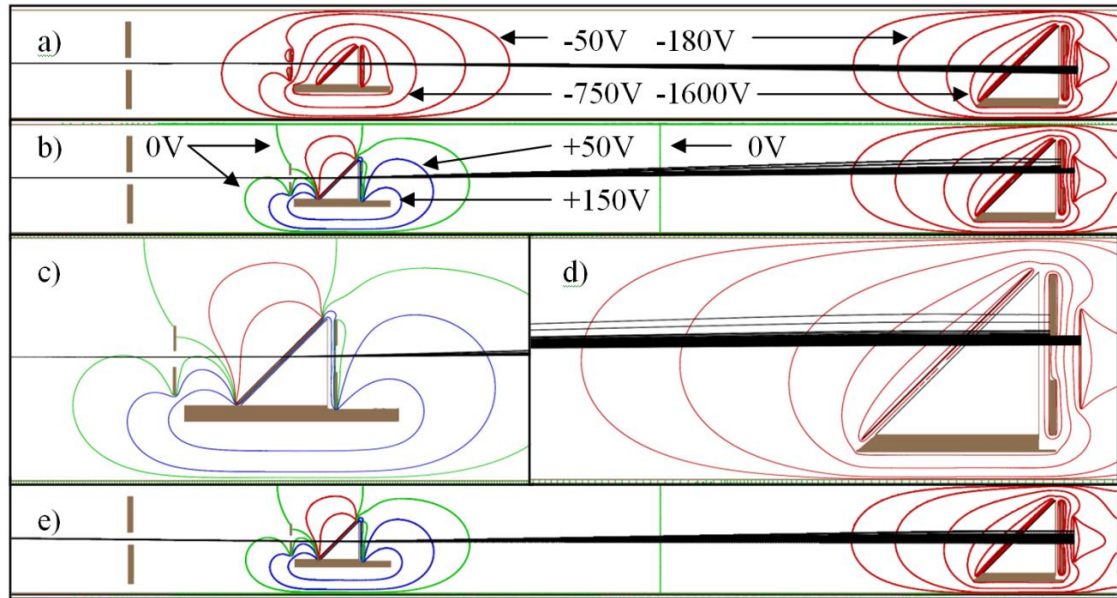
153

154 **3.1 Bending of the light ions due to timing gate voltages**

155

156 The bending of ion trajectories in the T1 timing gate was most prominent for the
157 hydrogen ions at the lowest simulated energies (50-150 keV). As can be seen from the
158 Fig. 2, the ion trajectories bend more when the T1 foil and mirror grid voltages are set to
159 0 V and -500 V, respectively (see Fig. 2 b, c and d) compared to the situation when the
160 foil and mirror are at -2800 V as in Fig. 2 a). This is because of the potential difference
161 over at mirror grids is smaller in the latter case (1000 V) compared to the first case (Fig.
162 2 b)), where the toblerone voltage is +1000 V (1500 V difference over mirror grids).

163



164

165 Figure 2. Bending of hydrogen ion trajectories in timing gates. Low energy hydrogen ion
 166 paths (initial energy 100 ± 50 keV) were simulated with SimION through the ToF-ERD
 167 spectrometer with E-detector being further right after the T2 timing gate. Red color:
 168 negative potential, green color: 0 V potential and blue color: positive potential. In a) both
 169 T1 and T2 have foil and mirror voltage at -2800 V and virtually field free toblerone part
 170 at -1800 V. In the rest of the figures the T1 foil is at the ground potential, the mirror at -
 171 500 V (to repel free electrons as in experimental setup) and the toblerone part for the T1
 172 at +1000 V. One can see that in b) and in the close-ups of c) and d) the hydrogen paths
 173 for lowest energies will not end up to the E-detector when the foil opening at T2 is 18 mm
 174 diameter. In e) 1% downward declination is used for incoming hydrogen ions with
 175 respect to the straight line of sight.

176 As seen from Fig. 2 d), the bending of the light ion trajectories can induce a reduction of
 177 the detection efficiency, which is already hindered due to the small stopping force and
 178 therefore small number of secondary electrons emitted by the lightest ions from carbon
 179 foils. However, this situation only occurs if the apertures before the first timing gate are
 180 limiting the solid angle too much. Example is given in Fig. 2 e) where incident ions that
 181 would not have hit the T2 detector originally are now bent in T1 towards the T2 detector.
 182 Due to this effect, if the first aperture(s) do not limit the solid angle too much, the number
 183 of missed ions, due to bending at T1, is compensated by the same number of ions that
 184 would have originally missed the T2 but are now bent towards it. This is the reason why
 185 the solid angle of the timing telescope should not be limited by the aperture(s) before the
 186 T1 foil.

187

188 3.2. Tandem effect in the timing gates

189

190 A charge state exchange in T1 foil will induce an energy spread to incident
 191 monoenergetic ions. The width of this spread caused by the tandem effect depend on

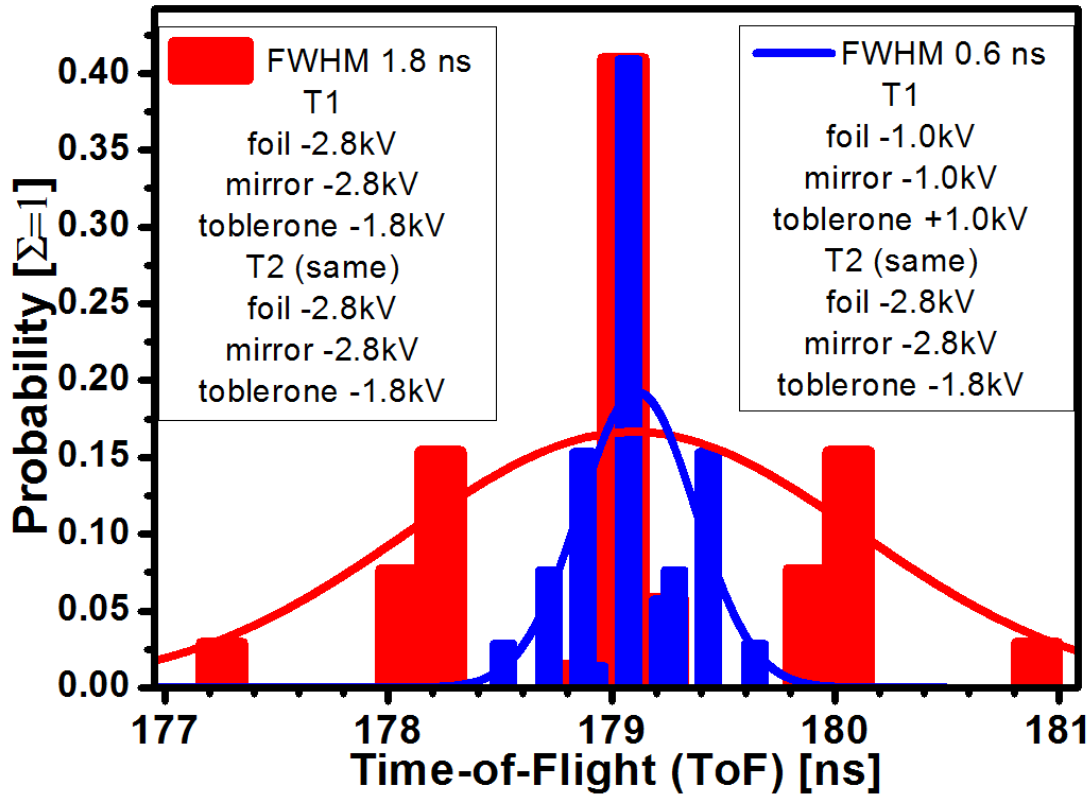
192 three main parameters: a) T1 timing gate foil voltage, b) the ion proton number (Z), c)
 193 velocity (energy) of specific ion. The charge state equilibrium and distribution which are
 194 reached at the T1 foil, are actually bound to the combination of b) and c). As shown later,
 195 timing gate orientation and other voltages than the one at T1 carbon foil have only a
 196 minor contribution to the magnitude of the tandem effect.

197
 198 The equilibrium charge state fraction F_q ($\sum_q F_q = 1$) defines the charge state probability
 199 of individual charge state before and after the foil. The width d of this charge state
 200 distribution over all charge states can be defined through the average charge state
 201 q_{av} ($= \sum_q q * F_q$) being $d^2 = \sum_q (q - q_{av})^2 * F_q$. The values q_{av} and d are the most
 202 usually reported values for the charge states distribution measurements for different ions
 203 and energies (or these can be calculated from the actual charge state distributions) [16].
 204

He energy [keV]	Charge state distribution			q_{av}	d
	2+	1+	0		
150	0.05	0.60	0.35	0.70	0.56
250	0.12	0.64	0.24	0.88	0.59
400	0.30	0.60	0.10	1.20	0.60
600	0.51	0.46	0.03	1.48	0.56
800	0.67	0.32	0.01	1.66	0.49

205 *Table I. Charge state fraction distribution of He after the carbon foil. Values estimated*
 206 *from a graph presented in [17]. q_{av} is the average charge state and d is the width (sigma)*
 207 *of the distribution (values calculated from the charge state distribution).*

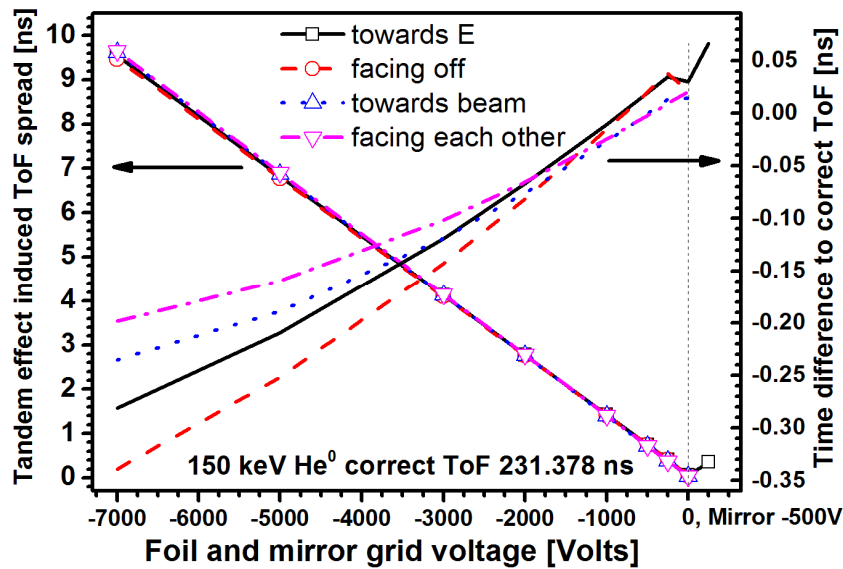
208 By knowing the fractions for different individual charge states F_q , the 9 different ToFs of
 209 the He form close to Gaussian shape when time-of-flights are simulated from the T1 foil
 210 to the T2 detector foil. The original charge states emerging from the sample can change
 211 in T1 foil and the resulting probability distribution of 9 different ToFs for the 250 keV He
 212 ions are shown in Fig. 3. Here, it can be seen from the Table I, that the central peak of the
 213 Gaussian shaped spread mainly forms from the 1+ to 1+ charge state exchange in the T1
 214 foil. T simulation results shown in Fig. 3 for two different T1 timing gate voltages, and
 215 T2 voltages kept the same, demonstrate that the ToF spread reduces for smaller T1 foil
 216 voltages.
 217



219

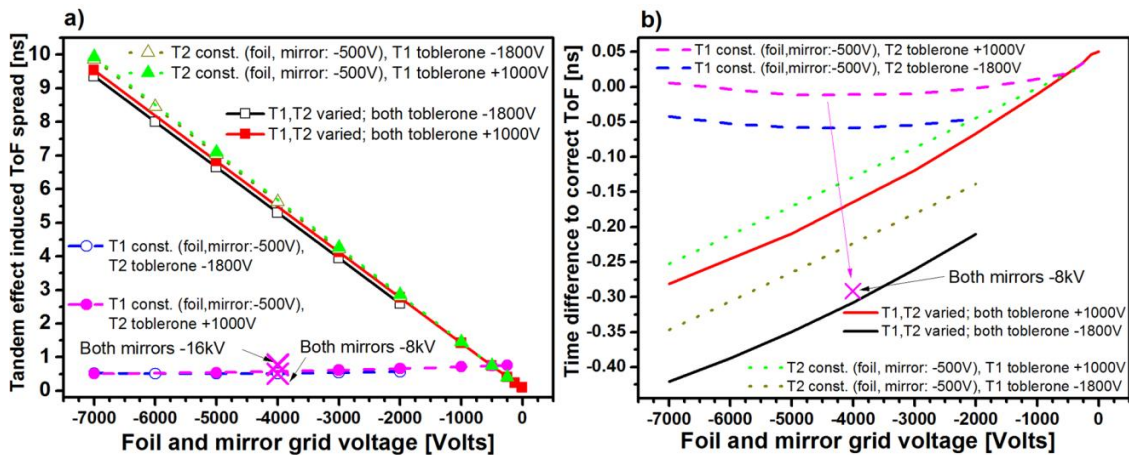
220 Figure 3. Simulated tandem effect induced time-of-flights for monoenergetic 250 keV He
 221 ions with three different charge states. Correct 250 keV He⁰ time-of-flight is 179.23 ns.
 222 Both timing gates faced towards the energy detector. Fractions for different charge states
 223 are taken from Table I. Fitted curves are pure Gaussian, FWHMs are calculated through
 224 weighted standard deviation σ obtained directly from the data.

225 In a similar manner as in Fig. 3, different timing gate orientations (see from Fig. 1) were
 226 simulated with varying foil and mirror voltages, in both timing gates same voltages were
 227 used. In practice, as can be seen from the Fig. 4, no differences in the magnitude (ToF
 228 spreading) of the tandem effect were observed between the four different timing gate
 229 orientations. However, small differences were observed when the peak position of the
 230 Gaussian fit of the different time-of-flights were compared. From this comparison, the
 231 timing gate orientation where foils faced towards each other suffered from the smallest
 232 position shift compared to the correct ToF of the selected energy. This shift of the peak
 233 position is however in practice always small compared to the magnitude of the simulated
 234 tandem effect. The spread induced by the tandem effect on the other hand can be close to
 235 5 % of ToF for low energies, if the foil voltages are pushed up to 7 kV(see Fig. 4).
 236



237

238 Figure 4. Impact of the timing gate orientation to the tandem effect induced ToF spread
 239 (left y-axis) and peak position shift (right y-axis). Both timing gates had the same
 240 voltages in all configurations. Simulated ion beam was 150 keV He and toberlone-part
 241 voltage was +1000 V for both timing gates. Timing gate orientation schematics can be
 242 seen from Fig. 1.



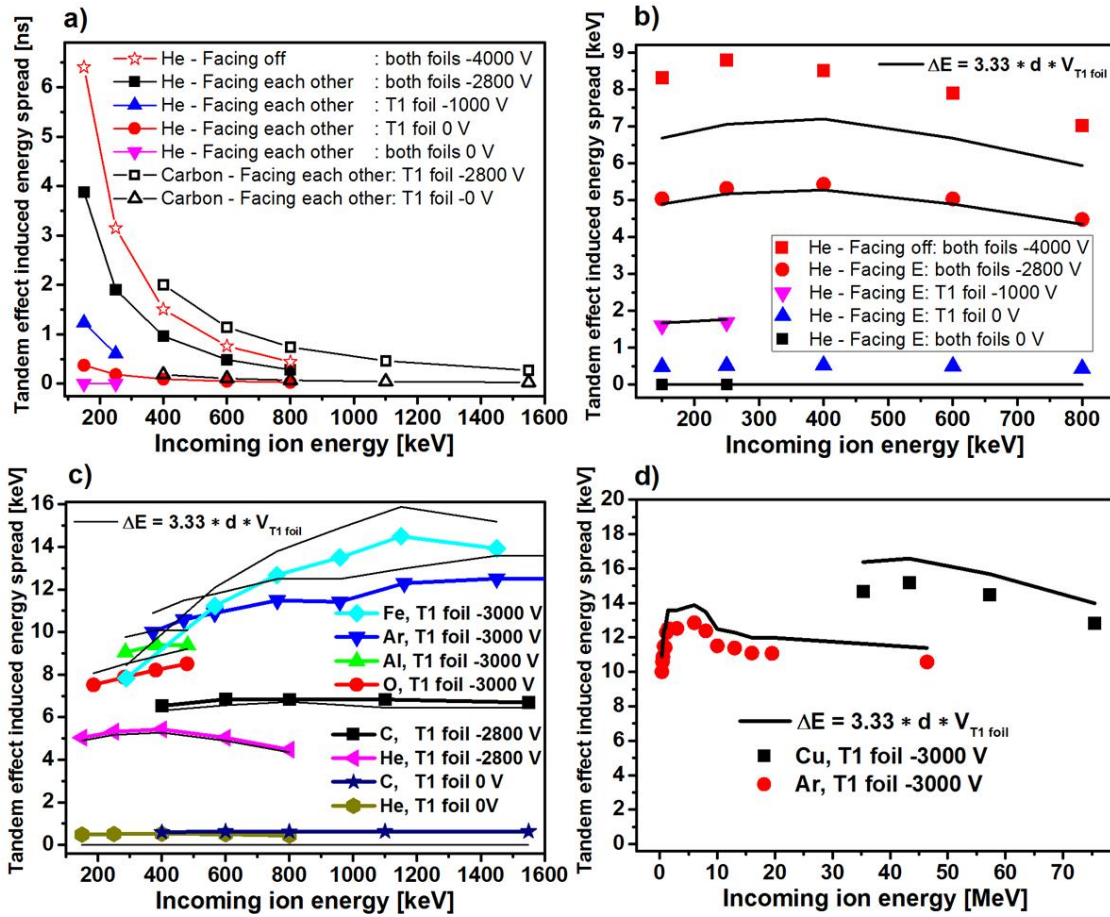
243

244 Figure 5. Impact of timing gate voltages to the tandem effect induced ToF spread (a) and
 245 peak position shift (b). In a) the simulated spread is given as FWHM. Simulated 150 keV
 246 He ions were used and correct ToF for He⁰ is 231.378 ns. The foil in both timing gates
 247 was facing towards the energy detector. Constant voltages in a) and b) refer to +1000 V
 248 in toberlone and -500 V in mirror and foil. Crosses where both mirrors are at high
 249 voltage, -8 kV or -16 kV, refer to the situation where T1 and both mirror voltages are
 250 constant and T2 foil voltage is -4000 V and toberlone +1000 V.

251 In Fig. 5, the voltage configurations of T1 and T2 were varied to see how much does the
252 T2 or mirror grid voltages influence the tandem effect. In situations where other timing
253 gate is said to be constant, say T1 is constant, only T2 foil and mirror voltage were
254 changed. In Fig. 5 a) the cases where T1 foil voltage is kept constant, the tandem effect is
255 small and causing less than 1 ns ToF spread even for the wide T2 foil voltage values. It
256 can also be noted that the two points marked in the same figure with text “both mirrors”
257 at -8 kV or -16 kV, do not influence the tandem effect in this timing gate configuration.
258 Mirror voltages can be seen to have an effect only at Fig. 5 b) where time difference to
259 the correct ToF is compared. Also, the toblorone part voltage has only a minor influence
260 to the tandem effect in both Fig. 5 a and b). In the Fig. 5 a) it is shown that when T1 foil
261 has the lowest voltages the tandem effect is small. At the bottom part of the same Fig. 5
262 a), however, it can be seen that the T2 voltages do have an influence to the velocity
263 (energy) profile of the passing ion when it flies between the two timing gates: for small,
264 constant T1 voltage, the higher the T2 voltage is the smaller the tandem effect is. It is
265 also clear that mirror grid voltages have no effect to the tandem effect but only the central
266 ToF peak position will change with increasing mirror voltages. This is due to
267 accelerating/decelerating effect of the T2 mirror grid (or also T1 depending on the gate
268 orientations) while the ion is between the timing gate foils.

269
270 To analyze the ToF (and energy) spread induced by the of the tandem effect deeper, ions
271 with different masses and energies were simulated with different timing gate orientations
272 and voltages. In Fig. 6 a) it is shown that for different energies and different timing gate
273 parameters the differences in the ToF spread values between the given situations stays
274 roughly constant over a wide energy range for the He ions as well as for C ions. When
275 simulated energy resolution (spread) for He and especially for heavier elements are
276 compared (see Figs. 6 b, c, d), certain constant pattern on the tandem effect behavior can
277 be seen. Fig. 6 b) shows that for the same ion (He) over a wide energy range the tandem
278 effect depends almost solely from the T1 foil voltage. In 6 c), the same linear dependence
279 can be observed, but now the Z of the ion sets the magnitude of the tandem effect when
280 the T1 foil voltage is kept constant. Finally when analyzing Fig. 6 d) the spread induced
281 by the tandem effect is not only a function of the T1 foil voltage and mass of the ion but
282 it follows almost hand-in-hand the width of the charge state distribution parameter d over
283 the very wide energy range, as can be expected.

284



285

286 Figure 6. Simulated resolution degradation in nanoseconds (a) and keVs (b, c and d) due to the tandem effect for different ion masses and beam energies. T1 mirror voltage is kept
 287 same as T1 foil and T1 toblorone being +1000 V while T2 voltages are the same as in Fig.
 288 2 and 3. The y-axis are in FWHM. Also an estimation for the tandem effect is shown in
 289 b), c) and d) as a solid line. The charge state fractions for different ions used in the
 290 simulations are taken from the following references: He [17], C [18], O [19], Al [19],
 291 Ar(< 1.5 MeV [18], > 1.5 MeV [20]), Fe [18], Cu [21].
 292

293 Values from the formula (1) estimating the magnitude of the tandem effect, are plotted to
 294 the Fig. 6 with single multiplier as an extra parameter

295

296

$$\Delta E_{\text{tandem effect}} = 3.33 * d * V_{T1 \text{ foil}}, \quad (1)$$

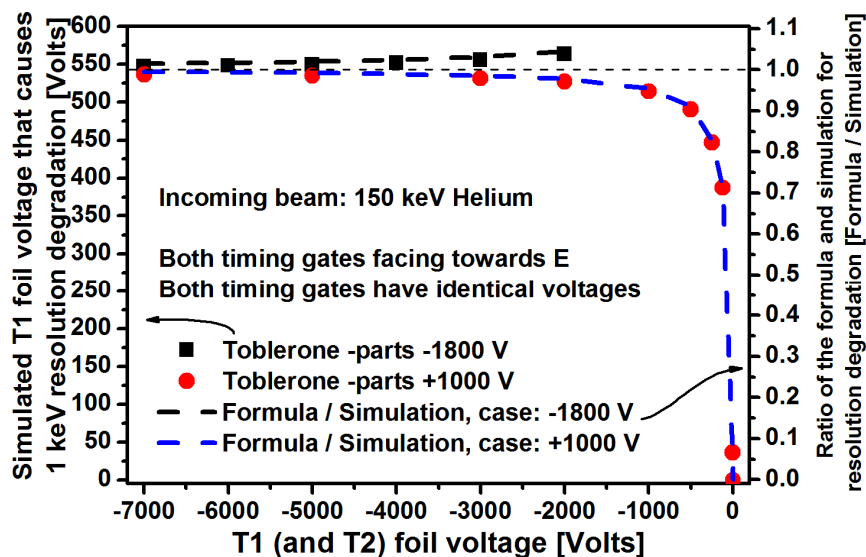
297

298 where d is the tabulated width (sigma) of the equilibrium charge state distribution at the
 299 specific energy (see from [16] for example), $V_{T1 \text{ foil}}$ is the T1 foil voltage in kV and
 300 $\Delta E_{\text{tandem effect}}$ [keV] is FWHM value of the energy spread when calculated from the ToF.
 301 The multiplier 3.33 comes from the $2.355 * \sqrt{2}$, where 2.355 is the factor to convert
 302 sigma, the value of d , to FWHM and $\sqrt{2}$ is the extra spreading caused when incoming ion
 303 charge state spread is quadratically summed with the charge state spread leaving from the

304 T1 foil. The simple linear formula does not preserve at T1 foil = 0 V or similar small
 305 values for T1 foil voltages, but it gives reasonable values for otherwise over a wide
 306 energy, mass and T1 foil voltage ranges. In Fig. 7 it is shown for the case of 150 keV He
 307 that the T1 foil voltage has close to linear dependence down to about 1000-500 V voltage
 308 but then, other voltages of the timing gates contribute more to the tandem effect. In a
 309 similar manner the estimate (1) used in the Fig. 7 drops below 80 % of the simulated
 310 values for T1 foil potentials smaller than -500 V.
 311

312 Although small resolution degradation is experimentally seen with He energy of 250 keV,
 313 +1000 V T1 toblerone voltages and maximum T1 foil voltage of -1200 V the higher
 314 energy data points did not gave concluding evidence. This was due to the measured
 315 resolution of about 5 keV with T1 foil voltage of 0 V for the 250 keV He ions measured
 316 with scattered beam from a thin Au film on Si substrate. The simulated data points in Fig.
 317 6 a) and b) for T1 foil voltage of 4 kV give comparable results to the experimental data
 318 presented in [2]. In this reference, for ~250 keV He ions the resolution was 3 keV when
 319 T1 foil was grounded and 12 keV when T1 foil was -4 kV.
 320

321 From the simulations presented, especially in the Fig. 6 d), it can be concluded that the
 322 average charge state q_{av} gives no contribution to the tandem effect (for example 75 MeV
 323 Cu used in Fig. 6 d) has average charge state q_{av} of 18.8+). This is due to the fact that
 324 incoming ions and those leaving from the T1 foil have the same average charge state and
 325 no practical velocity change occurs before/after the foil. For this reason all ions accelerate
 326 before the T1 foil and decelerate after it (or vice versa depending on the T1 foil polarity)
 327 thus gaining zero average net energy in the process. The only differences to the energy
 328 and thus to the ToF comes from the width d of the charge state distribution.



329

330 *Figure 7. T1 foil voltage dependence and the accuracy of the formulation. Left scale: T1*
 331 *foil voltage that causes 1 keV degradation to the simulated energy resolution. Right scale:*
 332 *a comparison between the formulation and the simulation in the T1 foil voltage range.*
 333 *Right scale scaled to 1.0 where T1 foil dependence is at linear region. 150 keV He beam*

334 was used with the timing gate configuration where both timing gates face towards the E
335 detector.

336

337 **4 Conclusions**

338

339 Two carbon foil time pick-up detectors were modeled using the real Jyväskylä ToF-ERD
340 spectrometer design in the SimION program to simulate the tandem effect. With the
341 simulations different timing gate orientations, voltages and ions and their energies were
342 tested. The tandem effect was found to be equal for all timing gate orientations. The
343 dominating factor, as identified also in the earlier publications was the T1 foil voltage,
344 while other voltages had impact to the tandem effect only when the T1 foil voltage was
345 less than -500 V. Simple formula to estimate the magnitude of the tandem effect was
346 found to fit the data on wide energy, ion mass and T1 foil voltage range. In this
347 estimation, the width d of the equilibrium charge state probability distribution and the T1
348 foil voltage both have a linear dependence to the magnitude of the tandem effect. The
349 bending of the low energy proton trajectories in the T1 mirror electric field can lead to the
350 situation where no protons reach the T2 foil if the solid angle of the detector is strictly
351 limited by the apertures before the T1 detector.

352

353

354

355

356 **Acknowledgements**

357

358 This work was supported under the auspices of Finnish Centre of Excellence Programme
359 2006-2014 (Project No. 213503, 251353 Nuclear and Accelerator Based Physics),
360 Finnish Funding Agency for Technology and Innovation (Tekes) project ALEBOND
361 (decision no. 40079/08), MECHALD (decision no. 40207/11) and HIUDAKE (decision
362 no. 70027/11) and Tekes EU-regional funds project (decision no. 70039/08).

363

364

365

References

366 [1] M.H. Mendenhall and R.A. Weller, Nucl. Instr. and Meth. B, 59 (1991), p. 120.

367 [2] M. Döbeli, R. Ender, V. Liechtenstein, D. Vetterli, Nucl. Instr. and Meth. B, 142
368 (1998), p. 417.

369 [3] Hamamatsu, *MCP & MCP assembly - selection guide*,
370 http://www.sales.hamamatsu.com/resources/pdf/etd/MCPassay_TMCP0001E09.pdf
371 (25.2.213).

372 [4] Tectra, *Microchannel Plates and Microchannel Plate Detectors*,
373 <http://www.tectra.de/MCP.htm> (25.2.1013).

- 374 [5] A. Zebelman, W. Meyer, K. Halbach, A. Poskanzer, R. Sextro, G. Gabor, D. Landis,
375 Nucl. Instr. and Meth., 141 (1977), p. 439.
- 376 [6] F. Busch, W. Pfeffer, B. Kohlmeyer, D. Schüll, F. Pühlhoffer, Nucl. Instr. and Meth.,
377 171 (1980), p. 71.
- 378 [7] Laitinen M., Rossi. M., Julin J., T. Sajavaara, Submitted to Nucl. Instr. and Meth. B,
379 (2013).
- 380 [8] C.G. Drexler and R.D. DuBois, Phys. Rev. A, 53 (1996), p. 1630.
- 381 [9] K. Arstila, T. Sajavaara, J. Keinonen, Nucl. Instr. and Meth. B, 174 (2001), p. 163.
- 382 [10] S. Giangrandi, T. Sajavaara, B. Brijs, K. Arstila, A. Vantomme, W. Vandervorst,
383 Nucl. Instr. and Meth. B, 266 (2008), p. 5144.
- 384 [11] Z. Siketic, I.B. Radovic, M. Jaksic, N. Skukan, Rev. Sci. Instrum., 81 (2010), p.
385 033305.
- 386 [12] Y. Zhang, B.D. Milbrath, W.J. Weber, M. Elfman, H.J. Whitlow, Appl. Phys. Lett.,
387 91 (2007), p. 094105.
- 388 [13] Simion 8.1, SIMION® Ion and Electron Optics Simulator, Scientific Instrument
389 Services, Inc.
- 390 [14] F. Grüner, F. Bell, W. Assmann, M. Schubert, Phys. Rev. Lett., 93 (2004), p.
391 213201.
- 392 [15] M. Kiisk, B. Erlandsson, M. Faarinen, R. Hellborg, K. Håkansson, P. Persson, G.
393 Skog, K. Stenström, Nucl. Instr. and Meth. A, 481 (2002), p. 1.
- 394 [16] N. Novikov and Y. Teplova, in *Journal of Physics: Conference Series* (IOP
395 Publishing, 2009), p. 082032.
- 396 [17] J. Armstrong, J. Mullendore, W. Harris, J. Marion, P. Phys. Soc., 86 (1965), p. 1283.
- 397 [18] P.L. Smith and W. Whaling, Phys. Rev., 188 (1969), p. 36.
- 398 [19] P. Hvelplund, E. Laegsgaard, J. Olsen, E. Pedersen, Nucl. Instr. and Meth., 90
399 (1970), p. 315.
- 400 [20] E.J. Knystautas and M. Jomphe, Phys. Rev. A, 23 (1981), p. 679.
- 401 [21] K. Shima, T. Ishihara, T. Miyoshi, T. Mikumo, Phys. Rev. A, 28 (1983), p. 2162.
- 402